Deformation of Cell Passing through Micro Slit between Micro Ridges Fabricated by Photolithography Technique

Yusuke TAKAHASHI, Shigehiro HASHIMOTO, Atsushi MIZOI, Haruka HINO

Biomedical Engineering, Department of Mechanical Engineering,
Kogakuin University, Tokyo, 163-8677, Japan
http://www.mech.kogakuin.ac.jp/labs/bio/

ABSTRACT

A micro slit has been designed between micro ridges, and deformation of a biological cell passing through the micro slit has been observed *in vitro*. The slit, of which the width is 0.87 mm and the height is 0.010 mm, has been made between the micro ridges on the transparent polydimethylsiloxane disk and on the glass disk by the photolithography technique. The slit is placed at the middle part of a flow channel. Four kinds of cells were used in the experiment: C2C12 (mouse myoblast cells), HUVEC (human umbilical vein endothelial cells), Hepa1-6 (mouse hepatoma cells), and Neuro-2a (mouse neural crest-derived cells). The suspension of each kind of cells was introduced to the slits. The deformation of cells passing through the micro slit was observed with an inverted phase-contrast microscope. The experimental results show that cells deform to the flat circular disk and pass through the micro slit of 0.010 mm height. The deformation ratio, the passing velocity, and the shape index of cells through the slit were evaluated: Hepa1-6 is deformed with the increase of the passing velocity, and HUVEC elongates along the flow. The designed slit between micro ridges has capability to evaluate the deformability of cells.

Keywords: Biomedical Engineering, C2C12, HUVEC, Hepa1-6, Neuro-2a, Photolithography and Micro-slit.

1. INTRODUCTION

The behavior of biological cells depends on the flow [1-22]. The deformability of the biological cell plays an important role *in vivo*.

An erythrocyte, for example, has high flexibility [1-8] and deforms in the shear flow [5, 6]. It also passes through micro-circulation, of which the dimension is smaller than the diameter of the red blood cell. After circulation through the blood vessels for days, the red blood cell is trapped in the microcirculation systems.

Several systems sort cells according to the deformability *in vivo*. One of the systems, which trap red blood cells, is a spleen. The spleen has special morphology in the blood flow path to sort injured red blood cells [7-9].

A slit is one of the systems, which sorts biological cells *in vivo*. The sorting at the slit depends on the deformability of the cell. Several cells are able to pass very narrow slits.

A photolithography technique enables manufacturing a micro-channel [1, 10-17]. Several micro-fabrication processes have been designed to simulate morphology of the microcirculation. The technique also will be applied to handle cells in diagnostics *in vitro*.

The photolithography technique can be applied to make a micro slit. The slit between micro cylinders was made to sort cells in the previous study.

The deformation of the depth direction between cylinders, however, cannot be observed by the conventional optical microscope. To observe the deformed cell at the direction perpendicular to the walls of the slit, the slit is designed with the combination of micro ridges in the present study.

In the present study, a micro slits have been fabricated between micro ridges by the photolithography technique, and deformation of a biological cell passing through the micro slit has been observed *in vitro*.

2. METHODS

Micro Slit

The slit, of which the width (*W*) is 0.87 mm and the height (*H*) is 0.010 mm, has been designed between a transparent polydimethylsiloxane (PDMS) disk and a borosilicate glass (Tempax) disk [1] (Fig. 1). Both of the disks have micro ridges. The upper disk of PDMS has a ridge of 0.06 mm height: 0.10 mm width, and 2 mm length. The lower disk of glass has two ridges of 0.3 mm width (2.3 mm length) with the interval (*W*) of 0.87 mm. These ridges make contact at the perpendicular position each other, and make slits between the ridges.

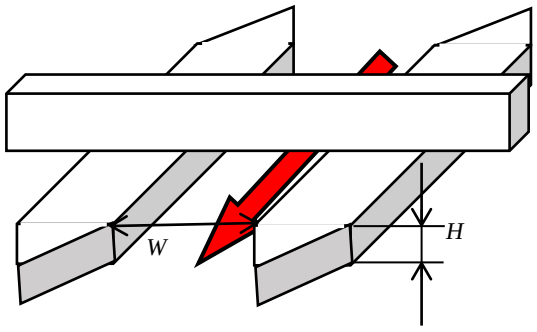

Fig. 1: Slit between ridges.

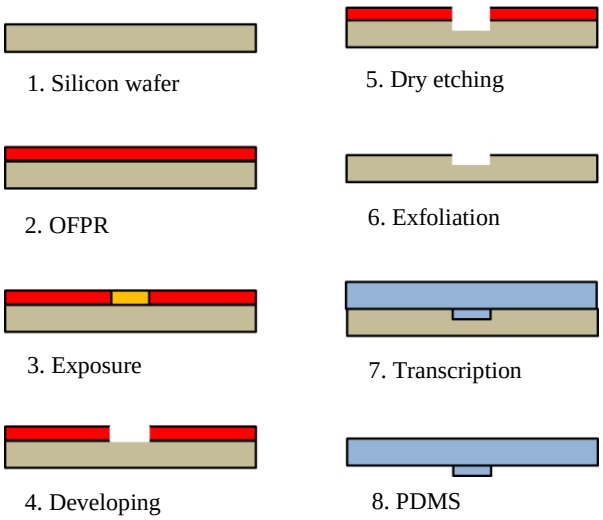

Fig. 2: Photolithography process of upper disk.

Upper Disk
A silicon wafer (Type N, Matsuzaki Seisakusyo, Co., Ltd., Tokyo, Japan) is used for a surface mold for the upper disk. The diameter and the thickness of the wafer are 50 mm and 0.30 mm, respectively (Fig. 2).

To improve affinity between the wafer and the photo-resist material, hexamethyldisilazane (HMDS, Tokyo Chemical Industry Co., Ltd., Tokyo, Japan) was coated on the wafer at 3000 rpm for 30 s with a spin coater (Mikasa Co., Ltd., Tokyo, Japan).

The positive photo-resist material of OFPR-800LB (Tokyo Ohka Kogyo Co., Ltd, Tokyo, Japan) was coated on the wafer at 3500 rpm for 5 s with the spin coater. The photo-resist was baked in an oven at 368 K for 3 min.

The pattern of ridges was drawn on the wafer by a laser (wave length of 405 nm) drawing system (DDB-201K-KH, Neoark Corporation, Hachioji, Japan). To increase the adhesiveness of the coating, the wafer was baked in the oven at 393 K for 5 min. The photo-resist was developed with tetra-methyl-ammonium hydroxide (NMD-3, Tokyo Ohka Kogyo Co., Ltd., Kawasaki, Japan).

The wafer was etched with the Deep RIE System (MUC-21 ASE-SRE, Sumitomo Precision Products Co., Ltd., Amagasaki, Japan) to make the deeper micro grooves. To exfoliate the residual photo-resist material from the surface, the disk was exposed to the oxygen gas of 30 milliliter per minute at power of 100 W for five minutes using a compact etcher (FA-1, Samco Inc., Kyoto): the oxygen plasma ashing.

The dimension of the grooves on the manufactured mold was measured by the laser microscope (VK-X200, Keyence Corporation, Osaka, Japan).

After the mold of the wafer was enclosed with a peripheral wall of polyimide, polydimethylsiloxane (PDMS: Sylgard 184 Silicone Elastomer Base, Dow Corning Corporation) was poured together with the curing agent (Dow Corning Corporation) on the wafer. The volume ratio of curing agent is ten percent of PDMS. The volume of PDMS is 8.8 cm^3 for the upper disk (4.5 mm thickness).

After degassing, PDMS was baked at 353 K for one hour in an oven (DX401, Yamato Scientific Co., Ltd, Tokyo, Japan). The baked disk of PDMS is exfoliated from the mold.

The dimension of the ridges on manufactured PDMS was measured with the laser microscope. The morphology of the ridge was observed by a scanning electron microscope (SEM, JSM6380LD, JEOL Ltd., Tokyo, Japan) (Fig. 4).

Two holes of 5 mm diameter were machined with a punching tool at the upper disk to make the inlet and the outlet for the flow channel.

Photomask for Lower Disk
The photomask was designed with two vacancies of 0.3 mm × 2.3 mm with the interval of 0.87 mm. The borosilicate glass (Tempax) disk (50 mm diameter, 1.1 mm thickness) was used for the base of the mask (Fig. 3). Before the vapor deposition of titanium, the surface of the glass plate was hydrophilized by the oxygen (30 cm^3/min, 0.1 Pa) plasma ashing for five minutes at 100 W by the reactive ion etching system (FA-1). Titanium was coated on the surface with 150 nm thick in the electron beam vapor deposition apparatus (JBS-Z0501EVC, JEOL Ltd., Japan). The positive photoresist material of OFPR-800LB was coated on the titanium at the disk at 7000 rpm for 20 s with the spin coater. The photoresist was baked in the oven at 338 K for five minutes.

The pattern was drawn on the mask with the laser drawing system. The pattern was baked on the heated plate at 368 K for five minutes. The photoresist was developed with NMD-3 for 5 minutes. The disk was rinsed by the ultrapure water, and dried by the spin-dryer. The titanium coating disk was etched with the plasma gas (SF_6, Ar) using RIE-10NR (Samco International, Kyoto, Japan).

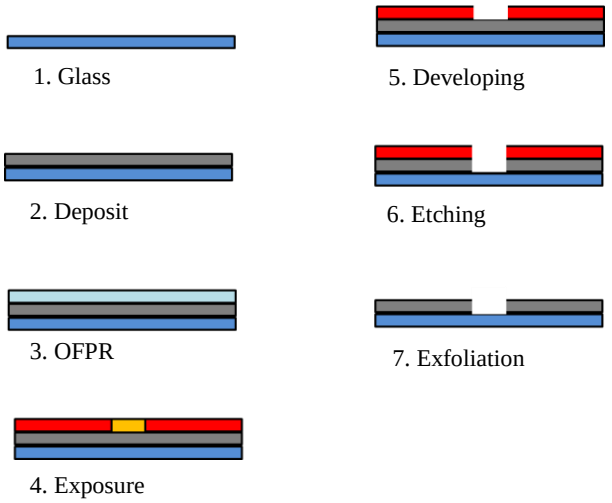

Fig. 3: Photo-mask for lower disk.

Lower Disk
The surface of the glass plate was hydrophilized by the oxygen (30 cm^3/min, 0.1 Pa) plasma ashing for five minutes at 100 W by the reactive ion etching system (FA-1) (Fig. 4). The negative photoresist material of high viscosity (SU8-10: Micro Chem Corp., MA, USA) was coated on the Tempax glass (50 mm diameter) at 2500 rpm for 30 s with a spin coater. The photo-resist was baked in the oven at 338 K for three minutes.

The photomask coated with titanium was adhered on the surface of SU8-10, and the photoresist was exposed to the UV light (90 mJ/cm^2) through the mask in the single sided mask aligner. After the resist was baked in the oven at 368 K for three minutes, the photoresist was developed with SU-8 developer (Nippon Kayaku Co., Ltd, Tokyo, Japan). The glass surface with the micro pattern was rinsed with IPA (2-propanol, Wako Pure Chemical Industries, Ltd.) for one minute, and with the ultrapure water for one minute. The plate was dried by the spin-dryer.

Flow Test System
A one-way flow system was designed to observe the behavior of cells through the micro slits *in vitro*. The system consists of a flow channel, a syringe pump, tubes and a microscope (Fig. 5). The micro-syringe-pump (Fusion200, CXF1020, ISIS Co., Ltd., Osaka) was used for the syringe pump. The silicone tube of 3 mm internal diameter and of 5 mm external diameter was used for the connector to the flow channel.

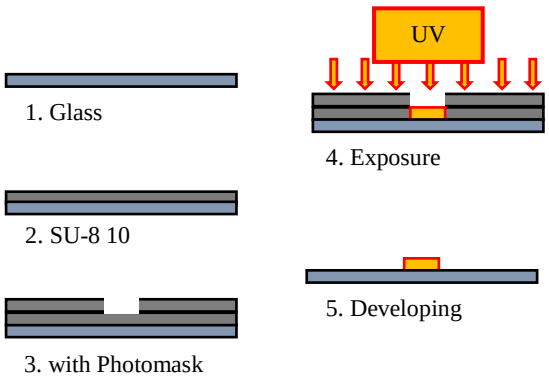

Fig. 4: Photolithography process of lower disk.

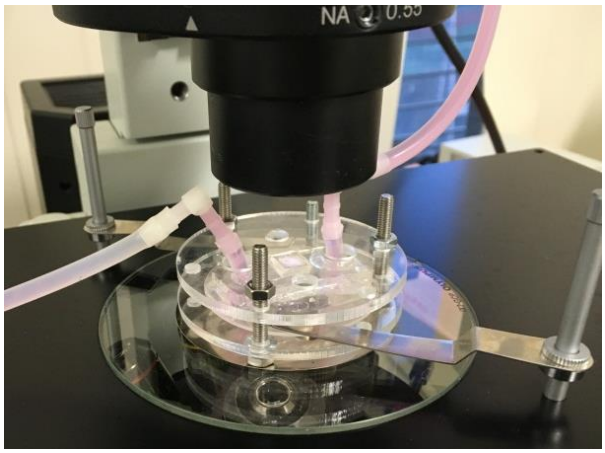

Fig. 5: Flow channel on microscope.

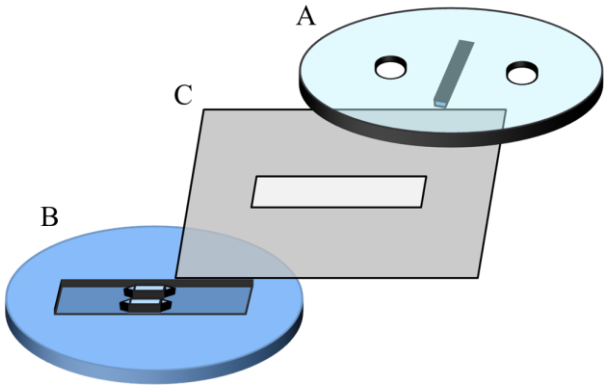

Fig. 6: Flow channel: upper PDMS (A) and lower glass (B) disks, and silicone sheet (C).

The flow channel consists of two transparent (upper and lower) disks and a thin sheet of silicone rubber (the thickness of 0.05 mm, ARAM Corporation, Osaka) (Fig. 6). A rectangular open space of 5 mm × 30 mm is cut off in the sheet, and sandwiched between the disks. The open space forms a channel of 30 mm length × 5 mm width × 0.05 mm depth. After hydrophilization by the oxygen plasma ashing for one minute at 100 W by the reactive ion etching system (FA-1), the three parts stick together with their surface affinity.

The lower PDMS disk has two micro ridges on the upper surface. The upper PDMS disk has one micro ridge on the lower surface. The upper disk has two holes. The silicone tubes are stuck at the holes for the inlet and the outlet. To seal the circumferential micro gap between disks, extra PDMS was painted to fill the gap from the outside, and baked at 373 K for one hour in the oven. The assembled flow chamber is sandwiched by two disks of poly-methyl-methacrylate to keep adherence between the parts to avoid leakage (Fig. 3).

Flow Test
Four kinds of cells (passage < 10) were used in the flow test: HUVEC (human umbilical vein endothelial cells), Hepa1-6 (mouse hepatoma cell line of C57L mouse), C2C12 (mouse myoblast cell line originated with cross-striated muscle of C3H mouse), and Neuro-2a (a mouse neural crest-derived cell line).

The cells were exfoliated from the bottom of the culture dish with trypsin or with the scraper (HUVEC), and suspended in the culture medium. After the saline solution was prefilled in the flow channel, the suspension of the cells was poured at the inlet of the flow channel.

The behavior of cells near the slit was observed with an inverted phase-contrast microscope (IX71, Olympus Co., Ltd., Tokyo), while the suspension of cells was introduced by the syringe pump at the flow rate of Q (1.4×10^{-10} $m^3/s < Q < 5.6 \times 10^{-10}$ m^3/s) or by the pressure difference (40 Pa) between inlet and outlet of the flow channel at 298 K. In the flow path of 0.05 mm height (5 mm width), the flow rate of 5.6×10^{-10} m^3/s makes the mean velocity of 2.0 mm/s.

The microscopic images of thirty frames per second at the shutter speed of 1/2000 s were captured by the camera (DSC-RX100M4, Sony). At the images, the outline of each cell was

traced with "Image J", and the area (A) was calculated. The deformation ratio was calculated as the ratio ($A_2 / A_1 > 1$) of the projected area of each cell before the slit (A_1) and that in the slit (A_2).

The velocity of the cell passing through the slit (v) was calculated every 1/30 second at the movie by "Kinovea". Most of cells pass through the slit in a few seconds, and Data of the clogging cell in the slit are not included in the following figures.

The counter of each projected area of HUVEC in the slit is approximated to the ellipsoid, and the shape index (R) is calculated by Eq. 1 (Fig. 11).

$$R = x / y \quad (1)$$

In Eq. 1, x is length of the minor axis, and y is length of the major axis of the ellipsoid. R is unity at the circle. R decreases, when the major axis increases as the elongation of the cell. At each cell, the angle (θ) between the major axis and the flow direction is measured. The angle (θ) is zero or 180 degree, when the major axis is parallel to the flow direction.

3. RESULTS

The tracing across the groove on the mold for the ridge of the upper disk measured by the laser microscope shows that the depth of the groove is 0.061 mm. The tracing across the ridge on the upper disk of PDMS measured by the laser microscope shows that the height of the ridge is 0.061 mm (Fig. 7).

Fig. 8 shows the morphology of the ridge observed by the scanning electron microscope: on the upper disk of PDMS, and on the lower disk of glass, respectively.

The tracing across the ridge on the lower disk measured by the laser microscope shows that the height of the ridge is 0.0105 mm (Fig. 9). Fig. 10 shows the micro slit between ridges observed by the inverted phase-contrast microscope.

Hepa 1-6 passing through the slit is exemplified in Fig. 11. The flow direction is from right to left in in Fig. 11. The vertical bar shows the ridge of PDMS of 0.1 mm width. The yellow line shows the tracing of the tergetted cell.

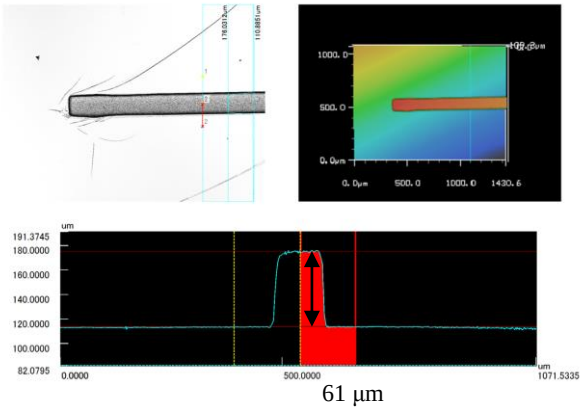

Fig. 7: Tracing across ridge on upper disk of PDMS measured by laser microscope: unit, µm.

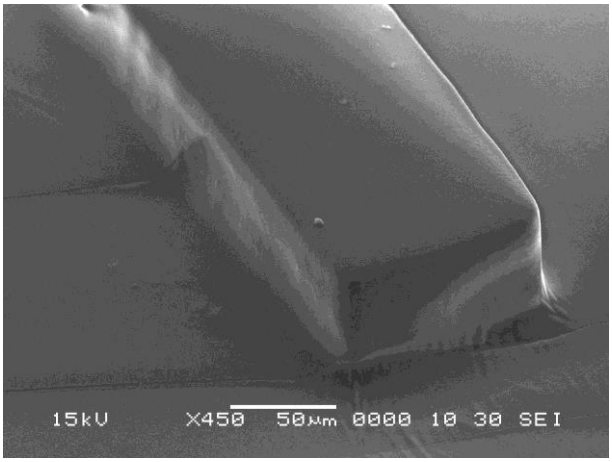

Fig. 8a: Morphology of ridge on upper disk of PDMS by SEM: bar shows 0.05 mm.

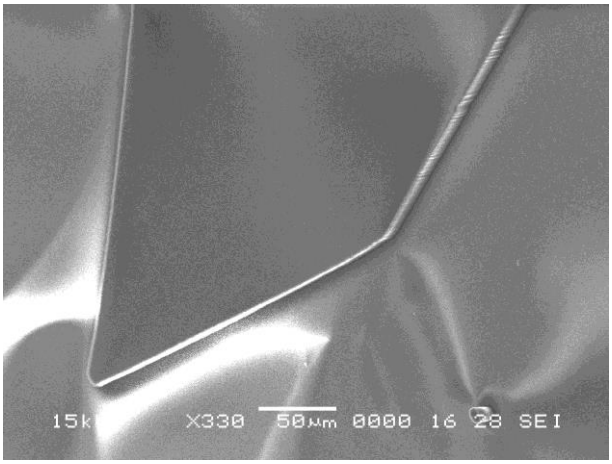

Fig. 8b: Morphology of ridge on lower disk of glass by SEM: bar shows 0.05 mm.

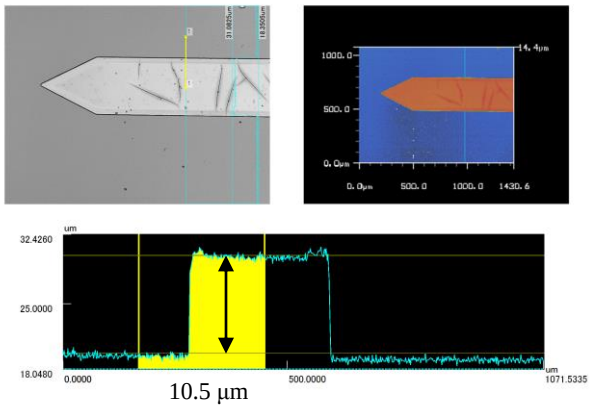

Fig. 9: Tracing across the ridge on the lower disk measured by laser microscope: unit, µm.

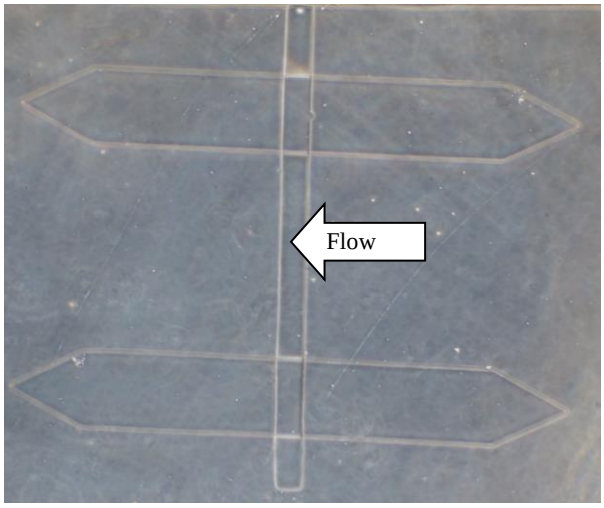

Fig. 10: Micro slit: dimension from left to right is 2.4 mm.

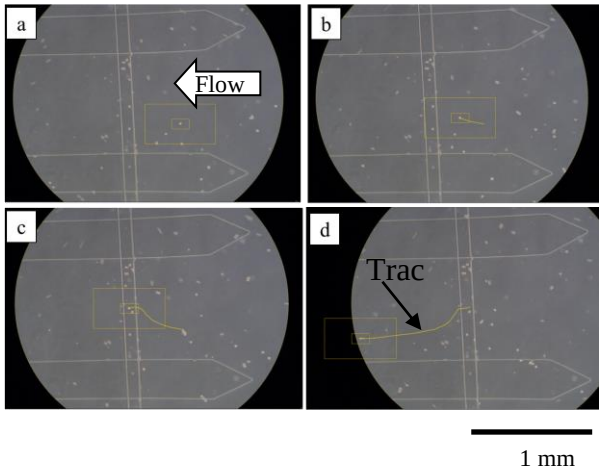

Fig. 11: Hepa1-6 flows through slit from right to left (a→d).

Fig. 12 shows the diameter of cell before passing through the slit. Fig. 12 shows no significant difference among the mean values of diameter of three kinds of cells. Several cells of Hepa1-6 have bigger diameters than those of the other kinds of cells.

Fig. 13 shows the projected area of HUVEC before slit (A_1) and that in the slit (A_2). The area of the same cell is connected by the line. The projected area of every cell increases in the slit ($A_1 < A_2$).

Data of the deformation ratio (A_2 / A_1) is plotted ascending order in Fig. 14. The mean value of deformation ratio at HUVEC is 1.21. The values of deformation ratio of Hepa1-6 scatter between 1.05 and 1.65, and split to low and high values. The mean value of (A_2 / A_1) at Hepa1-6 is 1.24 (Fig. 9).

Fig. 15 shows the relationship between the deformation ratio and the velocity of the cell. The velocity is low at Neuro-2a. Some cells of C2C12 pass the slit at higher velocity with the small deformation ratio. The deformation ratio tends to increase as the increase of the velocity of the cell (HUVEC, Hepa1-6), and the correlation coefficient is 0.2 and 0.8 at HUVEC (Fig. 15b) and Hepa1-6 (Fig. 15a), respectively.

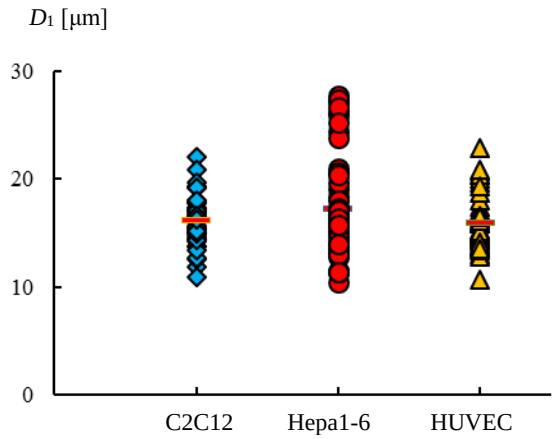

Fig. 12: Diameter (D) [μm] of cell: C2C12, Hepa1-6, and HUVEC: Bar shows mean.

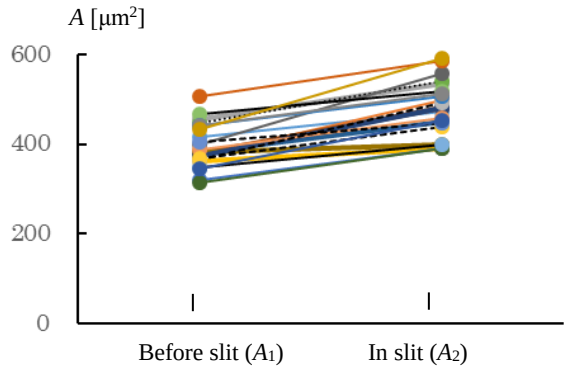

Fig. 13: Projected area of HUVEC [μm^2]: before slit (A_1; left), in slit (A_2; right).

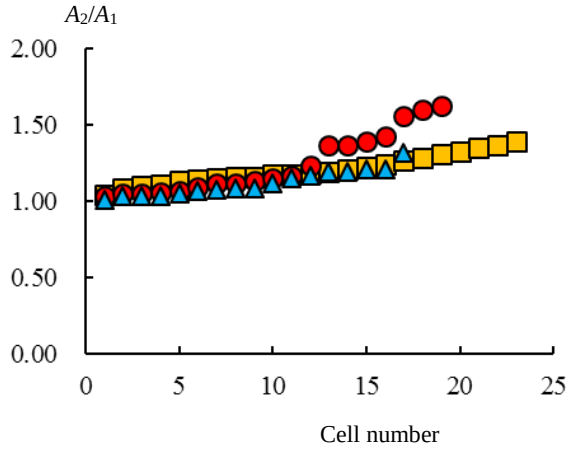

Fig. 14: Deformation ratio (A_2/A_1) of C2C12 (triangle), Hepa1-6 (circle), HUVEC (square).

Most of cells of HUVEC pass through the slit at constant speed. The values of the velocity of HUVEC distributes between 0.3 and 0.6 mm/s. The mean velocity of HUVEC passing through the slit is 0.45 mm/s.

Several cells of Hepa1-6 change the velocity during the flow through the slit in the present experiment. The values of the velocity of Hepa1-6 distributes between 0.2 and 0.9 mm/s. The mean velocity of Hepa1-6 passing through the slit is 0.52 mm/s. Most of cells are deformed to the circular disk to pass through the slit. Several cells of HUVEC, on the other hand, elongate along the stream line.

Fig. 16 shows the shape indexes (R) of 16 cells of HUVEC before (Fig. 11a) and during (Fig. 11b) passing through the slit. R decreases in many cells, which shows elongation of each cell in the slit.

Fig. 17 shows the angle (θ) between the major axis of each cell and the flow direction. The angle (θ) distribute at random before passing through the slit (Fig. 17a). In the slit, the angles (θ) concentrate around zero or 180 degree (Fig. 17b), which corresponds to the alignment of cells to the flow direction.

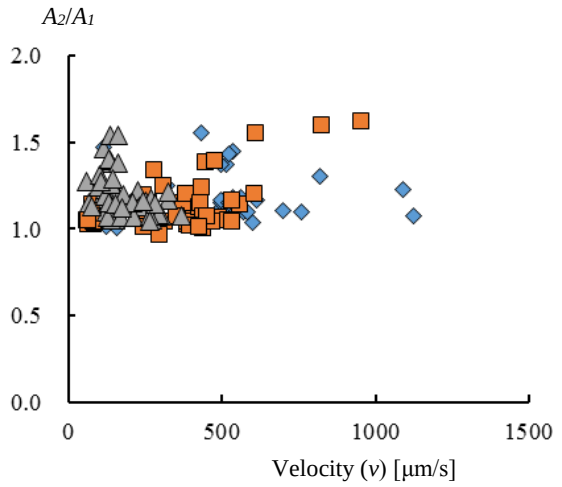

Fig. 15a: Cell velocity (v) [μm/s] vs. deformation ratio (A_2/A_1): C2C12 (rhombus), Hepa1-6 (square), Neuro2a (triangle).

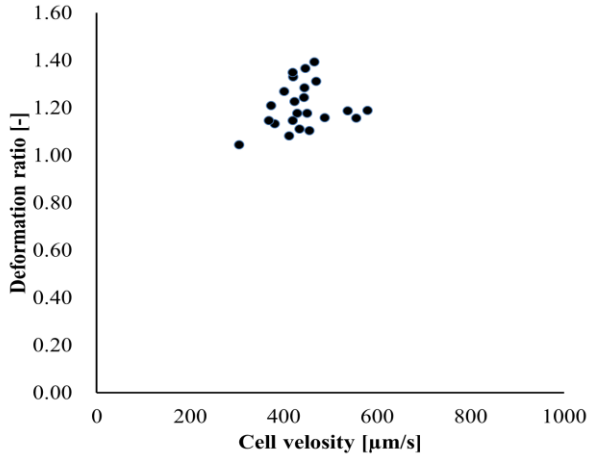

Fig. 15b: Relation between deformation ratio (A_2/A_1) and velocity of HUVEC passing through the slit (v).

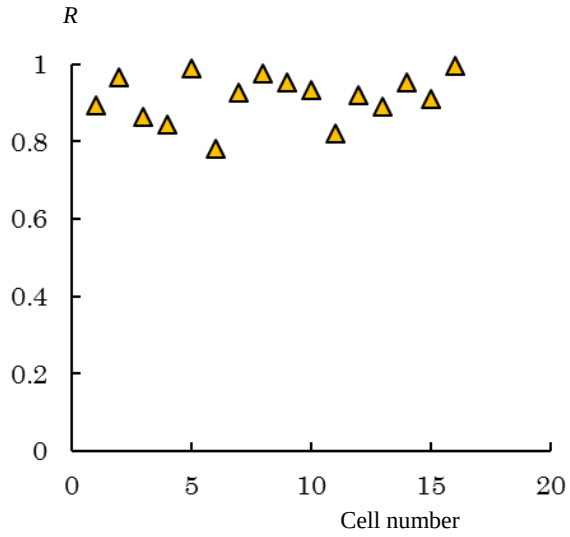

Fig. 16a: Shape index (R) of HUVEC before slit.

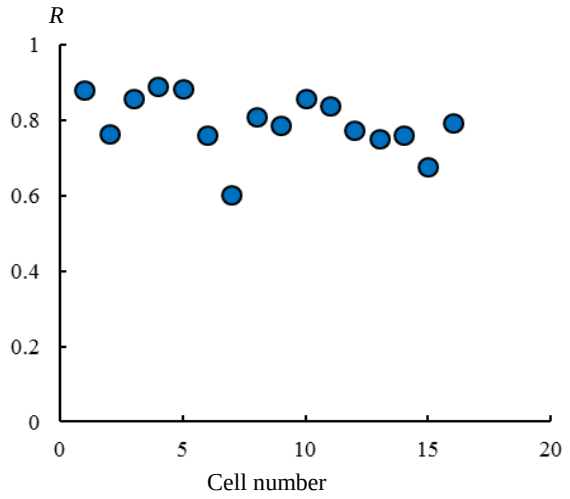

Fig. 16b: Shape index (R) of HUVEC in slit.

4. DISCUSSION

The lower ridge has the curvature of 0.01 mm at the tip of the side wall, which might reduce turbulence of the flow (Fig. 8b). Because the dimension of the slit is mainly governed by the height of the lower ridge in the present study, the slight over dimension of the height of the upper ridge does not vary the dimension of the slit. The ridge of the PDMS has elasticity, so that the micro ridge may deform with the small ratio.

The height of the slit (H = 0.010 mm) has been confirmed by the diameter of the cell (D), which passes through the slit.

$$3\pi D_1^3 / 32 = \pi D_2^2 H / 4 \qquad (2)$$

In Eq. 2, the volume of the cell is preserved: D_1 is the diameter before the slit, D_2 is the diameter in the slit.

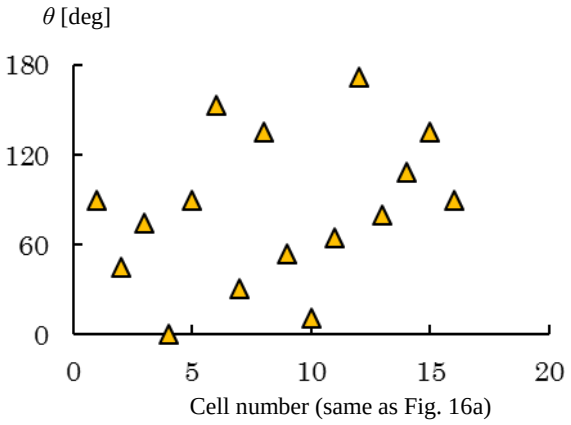

Fig. 17a: Angle (θ) [deg] of HUVEC before slit.

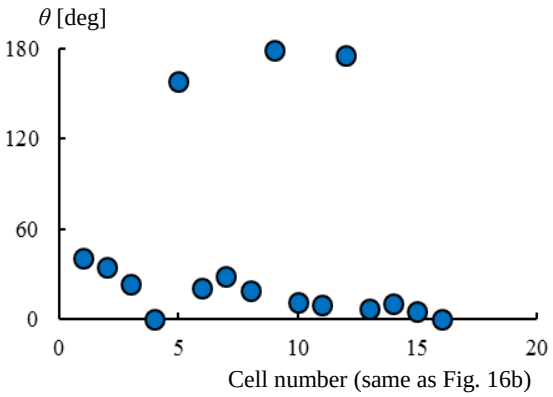

Fig. 17b: Angle (θ) of HUVEC in slit.

The height of the slit has been selected as the dimension slightly smaller than the diameter of the cell (C2C12, Hepa1-6, and HUVEC; Fig. 12). The dimension of the width of the slit has been selected 0.87 mm, which is enough wide for a cell to pass through. The wider width of the slit has possibility to make deformation of the wall, which could not keep precise dimension of the slit [1].

For the reason of the photolithography process, the edge of the ridge is not sharp, but it has an edge with a small width at the top. The biological system might have the sharper edge, so that a cell passes easily through the slit with the shorter travel distance *in vivo*. The cell has to struggle to pass through the slit in the present experimental device with the longer travel distance.

Adjusting the position of each micro ridge precisely on the counter plate is not easy. At the parallel position, a slit cannot be made, when the position shifts with the very short distance each other. To adjust easily the position of each micro ridge at the counter wall, the top of the ridges are set perpendicularly each other.

A biological cell has deformability. A biological cell shows not only passive deformation, but also active deformation [3]. The deformability of an erythrocyte has been studied related to the micro capillary [4].

The deformability of a cell depends on density of intra-cellular contents, which can be distinguished by the centrifuge [5]. While the cell passes through the slit, the cell keeps the circle shape at the shadow. The mean deformation ratio (A_2 / A_1) of red blood cell reported in the previous study is 1.31 [1].

The correlation coefficient is low between the velocity and the deformation ratio at RBC and at HUVEC. At Hepa1-6, on the other hand, the correlation coefficient is high.

HUVEC elongates to the direction of flow during the movement through the slit. RBC and Hepa1-6, on the other hand, are deformed into the flat circular disk during the movement through the slit. HUVEC elongates along the stream line on the blood vessel wall *in vivo*. Endothelial cells cover the inner surface of the vessel wall and are exposed to the blood flow every time *in vivo*. HUVEC might have high sensitivity to the flow direction especially with adhesion on the wall.

HUVEC might have the inner structure to elongate to the direction of the flow. Both C2C12 and Hepa1-6 might have the inner structure to keep the circular disk under the flow. Hepa1-6 might have high passive deformability to the moving velocity.

The moving velocity of the cell suspended in the media depends on the media velocity. In the present study, the flow rate of the suspension is not be controlled precisely by the syringe pump, because of several reasons: the compliance of the wall of the flow path, and clogging of the flow path. The flow is controlled by the pressure difference between inlet and outlet of the flow channel in the later part of the flow test, which has advantage to control inner pressure of the flow channel.

The moving velocity also depends on interaction between the cell and the surface of the slit (friction). To make the surface property stable, albumin is coated on the surface of the flow path in the present study.

The biological cells are sorted according to the shape, and deformability *in vivo*. Several cells pass through the micro slit. Some cells or fragments, which pass through the slit, are decomposed. Some cells, which cannot pass through the narrow channel, are captured, on the other hand.

An erythrocyte deforms from the biconcave disk to the parachute like shape, when it is passing through the micro capillary. An erythrocyte rotates in the shear field. The most of biological cells, on the other hand, keep the spherical shape, when they are flowing in the medium.

When passing through a micro slit, an erythrocyte deforms to the thin disk and struggles to go through. The mechanical property of the erythrocyte is maintained with energy consumption. To keep the biconcave shape, energy is consumed between structural proteins in the erythrocyte. The micro slit has been designed with the narrower dimension than that in the study with capillaries to observe the deformation of cells [15].

The fine architecture of the red pulp of the spleen was investigated in the previous studies [7-9]. In the previous studies, the typical diameter of the micro channel, which simulates the capillary blood vessel, was around 0.005 mm. The erythrocyte, on the other hand, passes through the micro slit narrower than 0.001 mm in the spleen.

The deformability of erythrocyte changes with aging [5]. The deformation is evaluated with the ratio of the projected area of the disk during the passing through the slit in the present study.

The deformation in the perpendicular direction can be observed with the slit between micro cylindrical pillars [10].

Some cells of HUVEC pass through the slit at the higher velocity with the small deformation ratio. Several bigger cells of Hepa1-6 pass through the slit at the higher velocity with the large deformation ratio.

5. CONCLUSION

The micro slits have been fabricated between micro ridges by the photolithography technique, and the deformation of a biological cell passing through the micro slit has been observed *in vitro*. The slit, of which the width is 0.87 mm and the height is 0.010 mm, has been designed between the ridge at the transparent polydimethylsiloxane disk and the ridges at the glass disk. The suspension of each kind of cells was introduced to the slits. The experimental results show that cells deform to the flat circular disk and pass through the micro slit. Hepa1-6 is deformed with the increase of the passing velocity, and HUVEC elongates along the flow. The designed slit between micro ridges has the capability to evaluate the deformability of cells.

6. ACKNOWLEDGMENT

This work was supported by a Grant-in-Aid for Strategic Research Foundation at Private Universities from the Japanese Ministry of Education, Culture, Sports and Technology.

REFERENCES

[1] A. Mizoi, Y. Takahashi, H. Hino, S. Hashimoto and T. Yasuda, "Deformation of Cell Passing through Micro Slit between Micro Ridges", **Proc. 20th World Multi-Conference on Systemics Cybernetics and Informatics**, Vol. 2, 2016, pp. 129-134.

[2] N. Mohandas, M.R. Clark, M.S. Jacobs and S.B. Shohet, "Analysis of Factors Regulating Erythrocyte Deformability", **The Journal of Clinical Investigation**, Vol. 66, No. 3, 1980, pp. 563-573.

[3] J.P. Brody, Y. Han, R.H. Austin and M. Bitensky, "Deformation and Flow of Red Blood Cells in a Synthetic Lattice: Evidence for an Active Cytoskeleton", **Biophysical Journal**, Vol. 68, No. 6, 1995, pp. 2224-2232.

[4] Y.C. Chen, G.Y. Chen Y.C. Lin and G.J. Wang, "A Lab-on-a-chip Capillary Network for Red Blood Cell Hydrodynamics", **Microfluidics and Nanofluidics**, Vol. 9, No. 2, 2010, pp. 585-591.

[5] S. Hashimoto, H. Otani, H. Imamura, et al., "Effect of Aging on Deformability of Erythrocytes in Shear Flow", **Journal of Systemics Cybernetics and Informatics**, Vol. 3, No. 1, 2005, pp. 90-93.

[6] S. Hashimoto, "Detect of Sublethal Damage with Cyclic Deformation of Erythrocyte in Shear Flow", **Journal of Systemics Cybernetics and Informatics**, Vol. 12, No. 3, 2014, pp. 41-46.

[7] L.T. Chen and L. Weiss, "The Role of the Sinus Wall in the Passage of Erythrocytes through the Spleen", **Blood**, Vol. 41, No. 4, 1973, pp. 529-537.

[8] G. Deplaine, I. Safeukui, F. Jeddi, F. Lacoste, V. Brousse, S. Perrot, S. Biligui, M. Guillotte, C. Guitton, S. Dokmak, B. Aussilhou, A. Sauvanet, D.C. Hatem, F. Paye, M. Thellier, D. Mazier, G. Milon, N. Mohandas, O. Mercereau-Puijalon, P.H. David and P.A. Buffet, "The Sensing of Poorly Deformable Red Blood Cells by the Human Spleen Can Be Mimicked in Vitro", **Blood**, Vol. 117, No. 8, 2011, pp. e88-e95.

[9] B. Steiniger, M. Bette and H. Schwarzbach, "The Open Microcirculation in Human Spleens: A Three-Dimensional Approach", **Journal of Histochemistry Cytochemistry**, Vol. 59, No. 6, 2011, pp. 639-648.

[10] Y. Takahashi, S. Hashimoto, H. Hino and T. Azuma, "Design of Slit between Micro Cylindrical Pillars for Cell Sorting", **Journal of Systemics, Cybernetics and Informatics**, Vol. 14, No. 6, 2016, pp. 8-14.

[11] Y. Takahashi, S. Hashimoto, H. Hino, A. Mizoi and N. Noguchi, "Micro Groove for Trapping of Flowing Cell", **Journal of Systemics, Cybernetics and Informatics**, Vol. 13, No. 3, 2015, pp. 1-8.

[12] A. Mizoi, Y. Takahashi, H. Hino, S. Hashimoto and T. Yasuda, "Deformation of Cell Passing through Micro Slit", **Proc. 19th World Multi-Conference on Systemics Cybernetics and Informatics**, Vol. 2, 2015, pp. 270-275.

[13] S. Hashimoto, A. Mizoi, H. Hino, K. Noda, K. Kitagawa and T. Yasuda, "Behavior of Cell Passing through Micro Slit", **Proc. 18th World Multi-Conference on Systemics Cybernetics and Informatics**, Vol. 2, 2014, pp. 126-131.

[14] S. Hashimoto, Y. Takahashi, H. Hino, R. Nomoto and T. Yasuda, "Micro Hole for Trapping Flowing Cell", **Proc. 18th World Multi-Conference on Systemics Cybernetics and Informatics**, Vol. 2, 2014, pp. 114-119.

[15] S. Hashimoto, T. Horie, F. Sato, T. Yasuda and H. Fujie, "Behavior of Cells through Micro Slit", **Proc. 17th World Multi-Conference on Systemics Cybernetics and Informatics**, Vol. 1, 2013, pp. 7-12.

[16] S. Hashimoto, R. Nomoto, S. Shimegi, F. Sato, T. Yasuda and H. Fujie, "Micro Trap for Flowing Cell", **Proc. 17th World Multi-Conference on Systemics Cybernetics and Informatics**, Vol. 1, 2013, pp. 1-6.

[17] H.W. Hou, Q.S. Li, G.Y.H. Lee, A.P. Kumar, C.N. Ong and C.T. Lim, "Deformability Study of Breast Cancer Cells Using Microfluidics", **Biomedical Microdevices**, Vol. 11, No. 3, 2009, pp. 557-564.

[18] B. Lincoln, H.M. Erickson, S. Schinkinger, F. Wottawah, D. Mitchell, S. Ulvick, C. Bilby and J. Guck, "Deformability-Based Flow Cytometry", **Cytometry, Part A: the journal of the International Society for Analytical Cytology**, Vol. 59, No.2, 2004, pp. 203-209.

[19] S. Hashimoto, F. Sato, H. Hino, H. Fujie, H. Iwata and Y. Sakatani, "Responses of Cells to Flow in Vitro", **Journal of Systemics Cybernetics and Informatics**, Vol. 11, No. 5, 2013, pp. 20-27.

[20] S. Hou, H. Zhao, L. Zhao, Q. Shen, K.S. Wei, D.Y. Suh, A. Nakao, M.A. Garcia, M. Song, T. Lee, B. Xiong, S.C. Luo, H.R. Tseng and H.H. Yu, "Capture and Stimulated Release

of Circulating Tumor Cells on Polymer-Grafted Silicon Nanostructures", **Advanced Materials**, Vol. 25, No. 11, 2013, pp. 1547-1551.

[21] A.W.L. Jay, "Viscoelastic Properties of the Human Red Blood Cell Membrane: I. Deformation, Volume Loss, and Rupture of Red Cells in Micropipettes", **Biophysical Journal**, Vol. 13, No. 11, 1973, pp. 1166-1182.

[22] C.L. Chaffer and R.A. Weinberg, "A Perspective on Cancer Cell Metastasis", **Science**, Vol. 331, No. 6024, 2011, pp. 1559-1564.